

RIDNet Assisted cGAN Based Channel Estimation for One-Bit ADC mmWave MIMO Systems

Erhan Karakoca^{*†‡}, Hasan Nayir^{*†‡}, Ali Görçin^{‡§}, Khalid Qaraqe^{*}

^{*} Department of Electrical and Computer Engineering, Texas A&M University at Qatar, Doha, Qatar

[†] Department of Electronics and Communication Engineering, Istanbul Technical University, İstanbul, Turkey

[‡] Communications and Signal Processing Research (HİSAR) Lab., TÜBİTAK BİLGEM, Kocaeli, Turkey

[§] Department of Electronics and Communication Engineering, Yildiz Technical University, İstanbul, Turkey

Emails: {karakoca19, nayir20}@itu.edu.tr, agorcin@yildiz.edu.tr, khalid.qaraqe@qatar.tamu.edu

Abstract—The estimation of millimeter-wave (mmWave) massive multiple input multiple output (MIMO) channels becomes compelling when one-bit analog-to-digital converters (ADCs) are utilized. Furthermore, as the number of antenna increases, pilot overhead scales up to provide consistent channel estimation, eventually degrading spectral efficiency. This study presents a channel estimation approach that combines a conditional generative adversarial network (cGAN) with a novel blind denoising network with a sparse feature attention mechanism. Performance analysis and simulations show that using a cGAN fused with a feature attention-based denoising neural network significantly enhances the channel estimation performance while requiring less pilot transmission.

Index Terms—channel estimation, one-bit ADC, massive MIMO, generative adversarial network, feature attention

I. INTRODUCTION

The millimeter-wave (mmWave) along with massive multiple input multiple output (MIMO) enables high-capacity communication for next-generation wireless mobile systems. However, massive MIMO systems bring additional complexity and cost to the overall system architecture. In particular, a large number of radio frequency (RF) chains and analog-to-digital converters (ADCs) used in massive MIMO systems significantly increase power consumption. This difficulty can be handled either by reducing the number of RF chains or utilizing one-bit analog-to-digital converter (ADC) [1]. The significant drawback of one-bit ADC is that the received signals are highly quantized, making channel estimation a challenging task. Therefore, high-accuracy and low-complexity estimation methods using minimal pilot overhead are needed for one-bit ADC massive MIMO systems.

Initial studies for massive MIMO channel estimation have been performed using compressive sensing (CS) methods based on approximate message passing (AMP) algorithms which exploit sparsity in mmWave channel [2], [3]. In practical scenarios, the performance of the AMP algorithm in channel estimation is bounded by the challenge of determining optimal shrinkage parameters. As another CS method, an expectation-consistent signal recovery algorithm has been proposed to model sparse mmWave channel elements using a Laplacian prior assumption [4], where the proposed technique outperforms AMP-based algorithms.

The CS methods require higher computational complexity and have lower performance compared to deep learning (DL) based approaches which have gained prominence for dealing with a wide range of channel estimation problems. For instance, learned denoising-based approximate message passing (LDAMP) [5] is proposed for mmWave beamspace channel estimation, where a denoising convolutional neural network (DnCNN) integrated with the AMP algorithm is utilized to reduce channel noise. Two-stage DL-based channel estimation techniques are common in mmWave MIMO systems when there are limited channel observations [6]–[9]. The unknown values of the channel matrix are predicted in the first stage, while the noise effects are reduced in the second stage. For example, a two-stage DL approach is employed to estimate channel state information in [6], where the unknown values of the channel matrix are estimated from the known pilot symbols using super-resolution (SR) network while image-restoration (IR) network is used to minimize the noise effect. Furthermore, another two-stage DL-based channel estimator is proposed in [7] for mmWave MIMO assuming that the number of antennas is lower than the number of pilots. The authors utilize a two-layer neural network and deep neural network (DNN) for pilot-aided channel estimation, while the second DNN is utilized for improving the channel estimation accuracy.

Recently, mmWave MIMO channel estimation is considered as a channel generation problem which is solved by using a generative adversarial network (GAN) in [10]. The loss functions of conventional DNNs are not well-suited for the one-bit MIMO channel estimation problem. Instead, experimentally tuned generic loss functions (i.e., \mathcal{L}_1 or \mathcal{L}_2) are utilized for DNNs. On the other hand, GANs allow designing a flexible loss function by learning the distribution of features belonging to the data adversarially. Most notably, a variation of GAN called conditional GAN (cGAN) [11], allows the model to generate samples conditioned on additional information by its loss function rather than generated randomly as in GANs. For example, cGAN can be used to generate samples of channel matrices using limited channel observations and pilot symbols, which helps yield more accurate channels. cGAN is applied for one-bit mmWave MIMO channel estimation in [12], and where the results reveal that cGAN outperforms even enhanced

CS methods and provide progress over DL-based channel estimation techniques.

Note that the above-mentioned DNN-based channel estimation methods have multiple stages. Although cGAN can provide slightly more accurate results over DNN-based approaches, the channel estimation ability can be further enhanced by employing a second stage. Considering that the observations are heavily quantized and reduced, the second stage can further decrease estimation errors across adjacent channel matrix components. In this paper, we propose a two-stage DL-based channel estimation technique inspired by both cGAN [13] and real image denoising network (RIDNet) [14], named cGAN-RIDNet. In the first stage, the coarse channel is reconstructed from highly quantized limited channel observations by having conditional input to cGAN and using two additional regularizations in the loss function. The second stage further enhances the channel matrix using RIDNet, significantly reducing noise from the coarsely estimated channel matrix. The numerical results show that RIDNet can successfully learn noise features in both spatial and angular domains. However, the channel estimation accuracy is higher when the RIDNet uses angular domain samples where the channel is represented sparsely. The cGAN-RIDNet provides almost identical performance results when the number of pilots is half that of the cGAN. The computational complexity of the RIDNet can be negligible compared to cGAN since its computational time is almost 1% of cGAN.

The remainder of this paper is structured as follows: Section II outlines the system model for a one-bit ADC mmWave MIMO channel, while Section III introduces the proposed cGAN-RIDNet architecture. Finally, Section IV presents simulation results, and Section V concludes the paper. Throughout the manuscript, we denote vectors using lowercase bold letters (e.g., \mathbf{x}), and matrices using uppercase bold letters (e.g., \mathbf{X}). The probability density function of the uniform distribution is denoted by \mathcal{U} . Additionally, $\mathcal{F}_x(\cdot)$ represents a function of the given subscript x . The superscript $*$ in text and figures denotes the sparse representation of the channel.

II. THE CHANNEL AND SYSTEM MODEL

We considered a mmWave massive MIMO system, where the base station (BS) has N RF chains and N antennas to serve K single-antenna user (UE) simultaneously as depicted in Fig. 1. Also, two one-bit ADCs are connected to each RF chain. The Saleh-Valenzuela channel model is employed to formulate the problem of one-bit ADC massive MIMO channel estimation. The spatial channel vector \mathbf{h}_k with size $N \times 1$ between the single UE and N -antenna BS can be expressed as

$$\mathbf{h}_k = \sqrt{\frac{N}{L_k}} \sum_{l=1}^{L_k} \alpha^{(k,l)} \mathbf{a}(\theta_{az}^{(k,l)}, \phi_{el}^{(k,l)}), \quad (1)$$

where L_k is the number of channel paths while $\alpha^{(k,l)}$, $\theta_{az}^{(k,l)}$, and $\phi_{el}^{(k,l)}$ indicate a complex gain, azimuth and elevation angles of l^{th} path, respectively. $\mathbf{a}(\theta_{az}^{(k,l)}, \phi_{el}^{(k,l)})$ denotes an

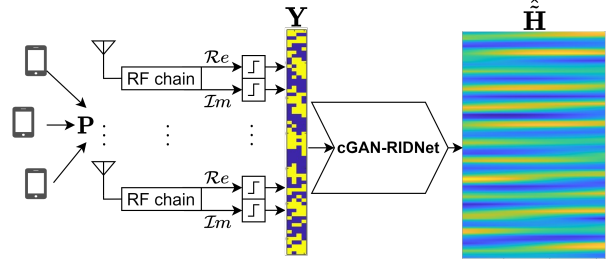


Fig. 1. System model and channel estimation stages where \mathbf{P} is pilot matrix, \mathbf{Y} is collected signal and $\hat{\mathbf{H}}$ is estimated channel.

antenna array response matrix which varies by array geometry. In this study, uniform linear array (ULA) is considered as follows

$$\mathbf{a}_{\text{ULA}}(\theta_{az}) = \frac{1}{\sqrt{N}} \left[e^{-j2\pi d \sin(\theta_{az}) \mathbf{n} / \lambda} \right], \quad (2)$$

where $\mathbf{n} = [0, 1, \dots, N-1]^T$, λ denotes wavelength, and $d = \lambda/2$ is antenna spacing. The spatial angles for the ULA can be defined as $\psi \triangleq d \sin(\theta_{az}) / \lambda$. Finally the spatial channel matrix $\mathbf{H} \in \mathbb{C}^{N \times K}$ for all UEs can be defined as

$$\mathbf{H} = [\mathbf{h}_1, \mathbf{h}_2, \dots, \mathbf{h}_k, \dots, \mathbf{h}_K]. \quad (3)$$

A spatial channel can be transformed into an angular domain by utilizing a discrete Fourier transform (DFT) matrix, which can be defined as

$$\mathbf{U} = [\bar{\mathbf{a}}_{\text{ULA}}(\bar{\psi}_{az}^1), \bar{\mathbf{a}}_{\text{ULA}}(\bar{\psi}_{az}^2), \dots, \bar{\mathbf{a}}_{\text{ULA}}(\bar{\psi}_{az}^N)]^H, \quad (4)$$

where $\bar{\psi}_{az}^n = \frac{1}{N} (n - \frac{N+1}{2})$ for $n = 1, 2, \dots, N$ is the grids for the angular domain which is predefined. Then, the mmWave channel in the angular domain can be defined as

$$\mathbf{H}^* = \mathbf{U}\mathbf{H}. \quad (5)$$

RIDNet can exploit the sparsity of the mmWave channel by learning sparse features better.

The UEs transmit a number of Q pilots to the BS during the training stage, and the received signal matrix $\mathbf{Y} \in \mathbb{C}^{N \times Q}$ using one-bit ADCs can be defined as

$$\mathbf{Y} = \text{sgn}(\mathbf{H}\mathbf{P} + \mathbf{N}), \quad (6)$$

where $\mathbf{P} \in \mathbb{C}^{K \times Q}$ is pilot matrix, $\mathbf{N} \in \mathbb{C}^{N \times Q}$ denotes noise matrix whose elements follow $\mathcal{CN}(0, \sigma_n^2)$, and $\text{sgn}(\cdot)$ is an element-wise signum function utilized for both real and imaginary components of its input x and defined as

$$\text{sgn}(x) = \begin{cases} 1 & , x \geq 0 \\ -1 & , \text{otherwise} \end{cases}. \quad (7)$$

An element of \mathbf{Y} can take any value from the given array $\{1+j, 1-j, -1+j, -1-j\}$.

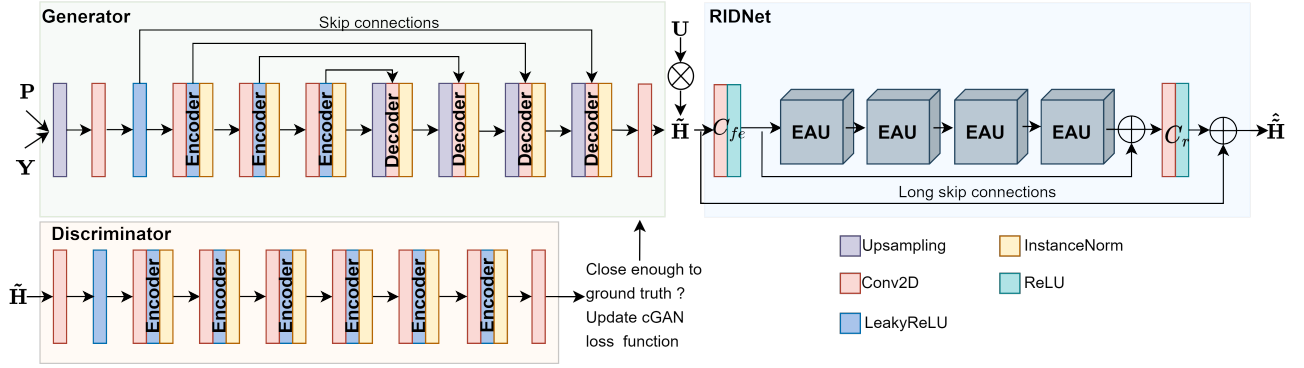


Fig. 2. Network architecture of the suggested cGAN-RIDNet method.

III. ONE-BIT ADC MIMO CHANNEL ESTIMATION ARCHITECTURE

In this section, the cGAN-RIDNet based one-bit ADC massive MIMO channel estimation method is introduced, which consists of two stages, namely cGAN and feature attention-based blind denoising network (RIDNet). In the first stage, the coarse mmWave channel $\hat{\mathbf{H}}$ is estimated from the received signal \mathbf{Y} by cGAN. The RIDNet in the second stage further enhances the channel estimation by reducing the noise effect over $\hat{\mathbf{H}}$ to obtain $\hat{\hat{\mathbf{H}}}$. The cGAN-RIDNet system architecture is shown in Fig. 2.

A. cGAN

A conventional GAN architecture consists of two competitive models: generator and discriminator. The generator task discovers a random mapping from noise to actual data while the discriminator evaluates if the generated data is real or not; by doing so, two models are trained adversarially. On the other hand, cGAN maps input samples to real data under given input conditions instead of random mapping. Our cGAN model is adopted from [13] with a modification in its loss function, where it is trained to discover the mapping relation between received signals \mathbf{Y} and a channel matrix \mathbf{H} , conditioned on pilot symbols \mathbf{P} .

1) *Generator*: The U-Net structure, which enables pixel-level features to be preserved at various resolutions by utilizing skip connections, is employed in the generator. To reconstruct the channel from the reduced observations, firstly, the input is scaled by an upsampling layer. Therefore, three encoder and four decoder blocks are utilized in U-Net. Each encoder and decoder block consists of convolutional and instance normalization layers. Convolutional layers of the decoders are used for upsampling of a given input to reconstruct the channel matrix, and instance normalization simplifies the learning process in generative models. One important thing is that the generator can over-optimize for a certain discriminator feature, and the discriminator can not improve. As a result, the generator only produces outputs with a small variation to convince the discriminator. This is referred to as a mode

collapse, and a \tanh activation function is used to prevent this phenomenon.

2) *Discriminator*: The patch structure is used in the discriminator, and it is composed of only convolutional layers. The patch structure is similar to a fully convolutional network. Different from the traditional discriminators, rather than generating one label as real or fake, patch structure allows analyzing the input as different patches and evaluates from these patches to determine if the generator output is real or fake. The patch structure consists of one convolutional layer with a *LeakyReLU* activation function at the beginning, and it is followed by four encoder blocks.

3) *Loss Function*: The primary goal of the cGAN is for the generator to learn how to generate the most natural channel matrix conditioned on the pilot symbol matrix. At the same time, the discriminator gains the ability to differentiate between produced and real channel matrices. Intuitively, the generator attempts to trick the discriminator by producing samples that appear indistinguishable from one another by optimizing the given loss function as

$$\mathcal{L}_{\text{cGAN}}(G, D, \mathbf{Y}, \mathbf{H}, \mathbf{P}) = \mathbb{E}[\log D(\mathbf{H}, \mathbf{P})] + \mathbb{E}[\log(1 - D(G(\mathbf{Y}, \mathbf{P})))] \quad (8)$$

G represents generator which aims to construct coarse channel matrices as $\hat{\mathbf{H}}$ and D denotes discriminator which aims to identify the generated channel $\hat{\mathbf{H}}$ from the actual channel \mathbf{H} . Thus, it is a min-max game between the generator and the discriminator, denoted as

$$\min_{\Psi} \max_{\Theta} \mathcal{L}_{\text{cGAN}}(G_{\Psi}, D_{\Theta}, \mathbf{Y}, \mathbf{H}, \mathbf{P}). \quad (9)$$

The generator aims to minimize this function, while the discriminator tries to maximize it by optimizing corresponding parameters Ψ and Θ , respectively.

The \mathcal{L}_1 and \mathcal{L}_2 regularizations are added to cGAN's loss function to generate a more realistic channel matrix, and they are expressed as

$$\mathcal{L}_1 = \mathbb{E}[\|\mathbf{H} - G(\mathbf{Y}, \mathbf{P})\|], \quad (10)$$

and

$$\mathcal{L}_2 = \mathbb{E}[\|\mathbf{H} - G(\mathbf{Y}, \mathbf{P})\|^2], \quad (11)$$

respectively. \mathcal{L}_1 regularization allows to retain of pixel-level details and makes the generated samples less blurry. However, it can cause sharp transitions between channel matrix elements. With \mathcal{L}_2 regularization, the discriminator's task remains the same; however, the generator is tasked to generate smoother samples. Thus, a good balance can be found to create a more realistic channel. The overall loss function becomes

$$\min_{\Psi} \max_{\Theta} \mathcal{L}_{cGAN}(G_{\Psi}, D_{\Theta}, \mathbf{Y}, \mathbf{H}, \mathbf{P}) + \lambda_1 \mathcal{L}_1 + \lambda_2 \mathcal{L}_2, \quad (12)$$

with λ_1 and λ_2 are weighting coefficients for \mathcal{L}_1 and \mathcal{L}_2 regularization, respectively

Following coarse reconstruction of the one-bit ADC MIMO channel matrix $\tilde{\mathbf{H}}$ from \mathbf{Y} and \mathbf{P} with cGAN, the estimated channel is transferred to the DL-based denoising network.

B. Feature Attention Based Blind Denoising Network

To enhance channel estimation performance, we utilized a feature attention-based blind denoising network. The formerly reconstructed channel with the cGAN is forwarded to the RIDNet whose architecture [14] consists of three key modules: the feature extraction module (C_{fe}), the feature learning residual on the residual module (R_{fl}), and the reconstruction module (C_r), respectively. The initial features from noisy channel matrix $\tilde{\mathbf{H}}$ can be extracted by using a feature extraction module, which consists of one convolutional layer and is represented as

$$f_{H_0} = C_{fe}(\tilde{\mathbf{H}}), \quad (13)$$

where $C_{fe}(\cdot)$ refers to the process of convolution performed on the input, and the resulting acquired features are denoted by f_{H_0} . Next, the extracted features are passed on to R_{fl} , which comprises four successive enhancement attention unit (EAU) units, each consisting of residual blocks with short and local skip connections. We will explain the role of this module later. By incorporating R_{fl} , the network can better learn the underlying patterns in the input data, which enables it to identify sparse features and estimate the noise in the channel matrix. This module can be represented as

$$f_{H_r} = R_{fl}(f_{H_0}), \quad (14)$$

where f_{H_r} denotes the explored features. Then f_{H_r} is summed up with the output of the first convolutional layer by long skip connection and forwarded to the reconstruction module, which consists only a convolutional layer $C_r(\cdot)$

$$\tilde{\mathbf{R}} = C_r(f_{H_r}). \quad (15)$$

To capture residual noise, the model uses a long skip connection that connects the network input to the output, as opposed to only mapping input data to a denoised output.

$$\hat{\mathbf{H}} = \tilde{\mathbf{H}} + \tilde{\mathbf{R}}, \quad (16)$$

where $\hat{\mathbf{H}}$ is the output of the whole network and represents the estimated channel.

The baseline characteristics can be managed to keep for the regression because of the utilized two long-skip connections

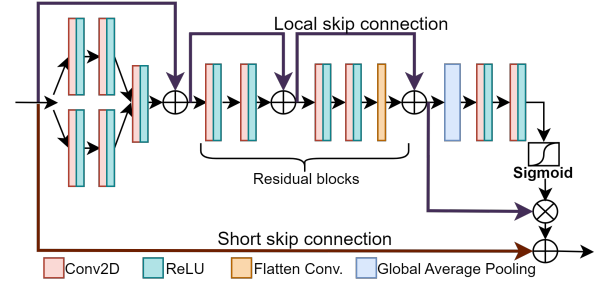


Fig. 3. The structure of the enhanced attention unit involves the utilization of two residual blocks. [14].

in the network, which allow initially obtained information to be conveyed directly to the end of the network. The loss function of the network for the given training set $\{\tilde{\mathbf{H}}_i, \mathbf{H}_i\}_{i=1}^M$, where the input for the RIDNet is the result of the conditional generative adversarial network (cGAN) and the label is the mmWave MIMO channel, can be expressed as

$$L(\mathcal{W}) = \frac{1}{M} \sum_{i=1}^M \left\| \mathcal{F}_{\text{RIDNet}}(\tilde{\mathbf{H}}_i) - \mathbf{H}_i \right\|_1, \quad (17)$$

where \mathcal{W} denotes all the trainable parameters of the network and \mathcal{F} denotes mapping function.

As a result, we can represent the final outcome of the proposed cGAN-RIDNet as

$$\hat{\mathbf{H}} = \mathcal{F}_{\text{RIDNet}}(\mathcal{F}_{\text{cGAN}}(\tilde{\mathbf{H}}; \mathbf{Y}, \mathbf{P})). \quad (18)$$

1) Enhanced Attention Unit: Two convolutional layers in the EAU are used to expand the pre-estimated features into two branches. The output of the branches is then concatenated and transmitted via a convolutional layer, which is followed by two consecutive residual blocks (RB). The first RB has two convolutional layers and allows the extraction of features, but the second RB has three convolutional layers and allows comprehension by flattening with an additional convolutional layer. It is worth noting that convolutional layers often allow for the extraction of local characteristics. After the residual blocks in the EAU module, a global average pooling layer is employed to retain the global features. This allows for the exploration of sparse channel features as well as inconsistencies in adjacent elements of the pre-estimated channel matrix. The global features are fed into two convolutional layers where the sigmoid activation function is used at the edge. The channel features captured at the end of the second residual block are multiplied with the result of the sigmoid activation function to utilize the statistics acquired through global average pooling, as described in [14]. By employing a short skip connection, the product of the multiplication is combined with EAU's input, enabling captured features and characteristics to flow between units.

IV. SIMULATIONS AND RESULTS

This section outlines the initialization settings and training strategies used for cGAN and RIDNet, followed by the presen-

tation of simulation results showcasing the effectiveness of the proposed approach. We assume $K = 32$, and each UE has an antenna. BS assumed to have $N = 64, 128, 192, 256$ antennas, which are connected to two one-bit ADCs to sample real and imaginary components of the received signal. Each UE channel is assumed to be composed of up to ten paths ($L_k = 10$). We set the remaining parameters of the channel in Eq. (1) for each UE as follows; for l^{th} path as $\alpha^{(k,l)} \sim \mathcal{CN}(0, 1)$, and $\theta_{az}^{(k,l)} \sim \mathcal{U}(-\frac{1}{2}\pi, \frac{1}{2}\pi)$.

A. cGAN-RIDNet Initialization

Each convolutional layer in the generator has 128 filters with 4×4 kernel size. Convolution layers in the discriminator contain 512 filters with 4×4 kernel size. Only the last layer of the discriminator contains a single filter to get an overall result from the patches.

Convolutional layers of the RIDNet have 64 filters and are unified with the *ReLU* activation function. The convolutional layers in the model have kernel sizes of 3×3 , except for the layer used to flatten inside the EAU, which has a kernel size of 1×1 . Four cascaded EAU modules were used for improved feature extraction.

B. Training

30×10^4 data pairs were used to train both networks for SNR values of $[-10, 20]$ by 5 dB margin, and for validation, %20 of the training data was reserved. The training data consist of two channels where the channels contain real and imaginary samples. cGAN model is trained using the MSProp algorithm with 2×10^{-4} and 2×10^{-5} learning rates for the generator and discriminator, respectively. In training RIDNet, the Adam optimizer is employed with an initial learning rate of 10^{-4} , which is later decreased to 10^{-5} during the training process, and eventually set to 10^{-6} to faster convergence. The TensorFlow framework is used to construct the network architecture and train the network offline. To investigate the effect of the sparse depiction of the mmWave channel, we also converted the initially estimated coarse channel matrix $\hat{\mathbf{H}}$ to angle domain $\tilde{\mathbf{H}}^* = \mathbf{U}\hat{\mathbf{H}}$ with DFT matrix \mathbf{U} . Then, the RIDNet also trained with transformed pairs $\{\tilde{\mathbf{H}}_i^*, \mathbf{H}_i^*\}_{i=1}^M$.

C. Comparison

The performance of the proposed method is assessed by employing the normalized mean square error (NMSE), as defined below

$$\text{NMSE(dB)} = 10 \times \log_{10} \left(\mathbb{E} \left\{ \frac{\|\hat{\mathbf{H}} - \mathbf{H}\|_2^2}{\|\mathbf{H}\|_2^2} \right\} \right). \quad (19)$$

We evaluated the NMSE of the proposed cGAN-RIDNet to that of cGAN for various pilot transmission instants (i.e., $Q = 2, 4, 6, 8$), and the results are presented in Fig. 4. Compared to cGAN, the employment of cGAN-RIDNet leads to a substantial enhancement in channel estimation performance across all SNR regimes for the same number of pilot transmissions $Q = 8$. With the suggested approach, it is possible to achieve the cGAN's channel estimation performance at 15

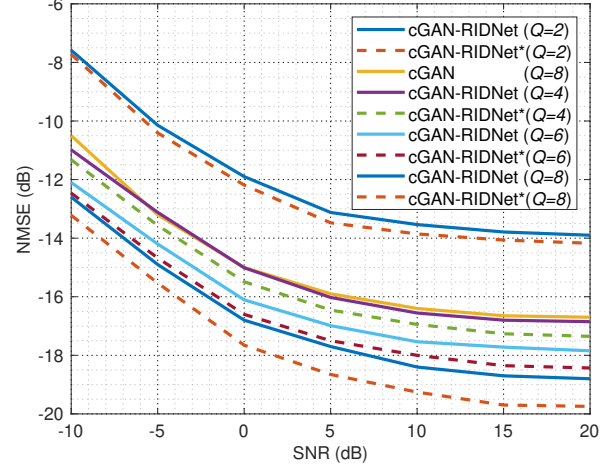


Fig. 4. The channel estimation performance comparison of the proposed method with different pilot transmissions.

dB SNR at about 1 dB SNR. Also, even when just half of the pilot transmission is used ($Q = 4$), the cGAN-RIDNet channel estimation performance almost exceeds the cGAN ($Q = 8$) performance. Furthermore, we investigated the effect of the sparse representation of the mmWave channel. It is analyzed that the RIDNet becomes more reliant and capable of disclosing features in the channel more effectively with this transformation because the RIDNet design can focus on sparse characteristics owing to its attention mechanism. Consequently, a straightforward transformation offers the suggested technique an additional channel estimation performance gain for all pilot transmissions. When there is only $Q = 2$ pilot transmission, the channel estimation performance of the proposed method degrades significantly. This is due to insufficient data to identify channel properties accurately.

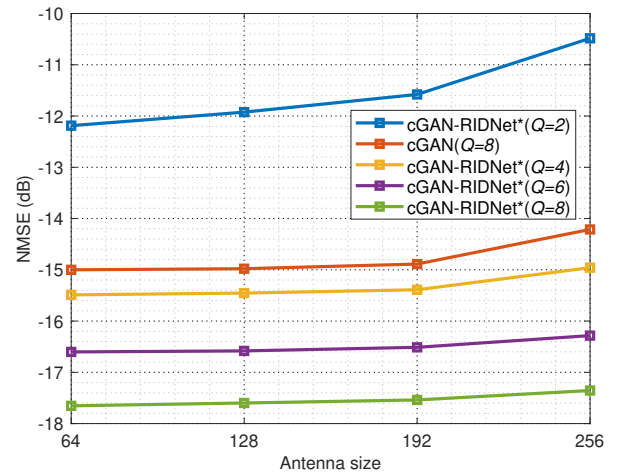


Fig. 5. Channel estimation performance for different antenna sizes.

We also evaluated the performance of the proposed method for the cases where the number of pilots is constant, but the number of antennas increases, as shown in Fig. 5. The channel

estimation performance of the proposed method significantly improves for all antenna sizes over the cGAN, even when only half of the pilot transmission is used. Even with a relatively modest pilot size ($Q = 4, 6, 8$), the performance of the cGAN-RIDNet remains reliable even when more antennas are installed at the BS.

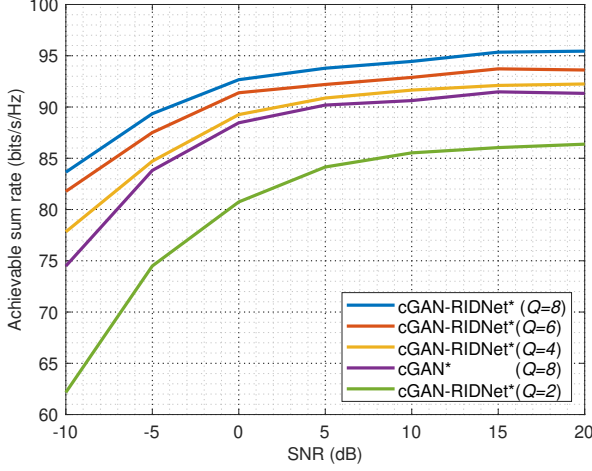


Fig. 6. The achievable sum rate for $K = 32$ UE with interference-aware beam selection scheme [15] under the proposed channel estimation method.

Furthermore, Fig. 6 demonstrates the achievable sum rate performance with the interference-aware beam selection scheme. As predicted by the previous findings, the proposed approach can achieve higher throughput using a lower pilot transmission overhead.

TABLE I
COMPUTATION TIMES OF THE NETWORKS

cGAN	RIDNET	cGAN-RIDNET
26.023 ms	0.2267 ms	26.2497 ms

Finally, the computation times of the cGAN and RIDNET networks separately and the proposed cGAN-RIDNet approach are presented in Table I. Since the RIDNet requires a significantly low computational load compared to the cGAN, the overall computation time of the cGAN-RIDNet is quite close to the cGAN. Considering the accuracy improvement for the channel estimation performance by the cGAN-RIDNET, this minor increase in the computation time is a reasonable compromise, and the proposed method can be used in practical scenarios.

V. CONCLUSION

Our focus was on investigating the issue of estimating the mmWave MIMO channel in situations where the BS employs one-bit ADCs. The channel estimation performance of the one-bit mmWave MIMO can be improved by employing cGAN-RIDNET, which is leveraged by both cGAN and the feature attention-based blind denoising network. The numerical results demonstrate that the proposed method significantly enhances the channel estimation accuracy using a lower pilot overhead while computation time is kept comparable.

ACKNOWLEDGMENT

This publication was made possible in parts by NPRP13S-0130-200200 and by NPRP14C-0909-210008 from the Qatar National Research Fund (a member of The Qatar Foundation). The statements made herein are solely the responsibility of the authors. We thank to StorAIge project that has received funding from the KDT Joint Undertaking (JU) under Grant Agreement No. 101007321. The JU receives support from the European Union's Horizon 2020 research and innovation programme in France, Belgium, Czech Republic, Germany, Italy, Sweden, Switzerland, Türkiye, and National Authority TÜBİTAK with project ID 121N350.

REFERENCES

- [1] Y. Li, C. Tao, G. Seco-Granados, A. Mezghani, A. L. Swindlehurst, and L. Liu, "Channel estimation and performance analysis of one-bit massive mimo systems," *IEEE Transactions on Signal Processing*, vol. 65, no. 15, pp. 4075–4089, 2017.
- [2] J. Mo, P. Schniter, N. G. Prelcic, and R. W. Heath, "Channel estimation in millimeter wave mimo systems with one-bit quantization," in *2014 48th Asilomar Conference on Signals, Systems and Computers*. IEEE, 2014, pp. 957–961.
- [3] J. P. Vila and P. Schniter, "Expectation-maximization gaussian-mixture approximate message passing," *IEEE Transactions on Signal Processing*, vol. 61, no. 19, pp. 4658–4672, 2013.
- [4] R. Wang, H. He, S. Jin, X. Wang, and X. Hou, "Channel estimation for millimeter wave massive mimo systems with low-resolution adcs," in *2019 IEEE 20th International Workshop on Signal Processing Advances in Wireless Communications (SPAWC)*. IEEE, 2019, pp. 1–5.
- [5] H. He, C.-K. Wen, S. Jin, and G. Y. Li, "Deep learning-based channel estimation for beamspace mmwave massive mimo systems," *IEEE Wireless Communications Letters*, vol. 7, no. 5, pp. 852–855, 2018.
- [6] M. Soltani, V. Pourahmadi, A. Mirzaei, and H. Sheikhzadeh, "Deep learning-based channel estimation," *IEEE Communications Letters*, vol. 23, no. 4, pp. 652–655, 2019.
- [7] C.-J. Chun, J.-M. Kang, and I.-M. Kim, "Deep learning-based channel estimation for massive mimo systems," *IEEE Wireless Communications Letters*, vol. 8, no. 4, pp. 1228–1231, 2019.
- [8] Y. Wei, M.-M. Zhao, M. Zhao, M. Lei, and Q. Yu, "An amp-based network with deep residual learning for mmwave beamspace channel estimation," *IEEE Wireless Communications Letters*, vol. 8, no. 4, pp. 1289–1292, 2019.
- [9] Q. Ji, C. Zhu, and X. Guo, "mmwave mimo: An lamp-based network with deep residual learning combining the prior channel information for beamspace sparse channel estimation," in *2021 IEEE 21st International Conference on Communication Technology (ICCT)*. IEEE, 2021, pp. 279–284.
- [10] E. Balevi and J. G. Andrews, "Wideband channel estimation with a generative adversarial network," *IEEE Transactions on Wireless Communications*, vol. 20, no. 5, pp. 3049–3060, 2021.
- [11] M. Mirza and S. Osindero, "Conditional generative adversarial nets," *arXiv preprint arXiv:1411.1784*, 2014.
- [12] Y. Dong, H. Wang, and Y.-D. Yao, "Channel estimation for one-bit multiuser massive mimo using conditional gan," *IEEE Communications Letters*, vol. 25, no. 3, pp. 854–858, 2020.
- [13] P. Isola, J.-Y. Zhu, T. Zhou, and A. A. Efros, "Image-to-image translation with conditional adversarial networks," in *Proceedings of the IEEE conference on computer vision and pattern recognition*, 2017, pp. 1125–1134.
- [14] S. Anwar and N. Barnes, "Real image denoising with feature attention," in *Proceedings of the IEEE/CVF international conference on computer vision*, 2019, pp. 3155–3164.
- [15] X. Gao, L. Dai, Z. Chen, Z. Wang, and Z. Zhang, "Near-optimal beam selection for beamspace mmwave massive mimo systems," *IEEE Communications Letters*, vol. 20, no. 5, pp. 1054–1057, 2016.